催化学报
2012 Chinese Journal of Catalysis Vol. 33 No. 4

Article ID: 0253-9837(2012)04-0583-12 **DOI**: 10.1016/S1872-2067(11)60359-8 **Review:** 583–594

Development of Ni-Based Catalysts for Steam Reforming of Tar Derived from Biomass Pyrolysis

Dalin LI[1,2], Yoshinao NAKAGAWA[1], Keiichi TOMISHIGE[1,*]

[1]*Department of Applied Chemistry, School of Engineering, Tohoku University, Sendai 980-8579, Japan*

[2]*National Engineering Research Center of Chemical Fertilizer Catalyst, Fuzhou University, Fuzhou 350002, Fujian, China*

Abstract: Nickel catalysts are effective for the steam reforming of tar derived from biomass pyrolysis, but the improvement is needed in terms of activity, stability, suppression of coke deposition and aggregation, and regeneration. Our recent development of Ni-based catalysts for the steam reforming of tar is reviewed including the modification with CeO_2 (or MnO), trace Pt, and MgO. The role of additives such as CeO_2, MnO, Pt, and MgO is also discussed.

Key words: steam reforming; tar; biomass; nickel; ceria; manganese oxide; platinum; magnesia

CLC number: O643 **Document code:** A

Received 30 October 2011. Accepted 14 December 2011.

**Corresponding author. Tel: +81-22-795-7214; Fax: +81-22-795-7214; E-mail: tomi@erec.che.tohoku.ac.jp*

This work was supported by Japan Science and Technology Agency (JST), Ministry of Education, Culture, Sports, Science and Technology, Japan.

English edition available online at Elsevier ScienceDirect (http://www.sciencedirect.com/science/journal/18722067).

Conversion of biomass to synthesis gas and hydrogen is one of the important technologies for the energy utilization of biomass by the power generation and the production of liquid fuels by Fischer-Tropsch synthesis and chemicals by methanol synthesis [1–4]. The gasification of biomass to synthesis gas and hydrogen has been conventionally carried out in a non-catalytic system at very high temperature (> 1073 K) in order to decrease the concentration of the residual tar [4]. In the non-catalytic gasification, air is usually used as a gasifying agent. Therefore, the product gas is diluted with nitrogen and this makes the product gas unsuitable to the chemical conversion. Another gasification method is the catalytic steam reforming of tar derived from the pyrolysis of biomass at much lower temperature than the case of non-catalytic gasification with air. It has been known that rapid pyrolysis at low temperature such as 773 K gives high yield of the mixture of volatile organic compounds, which is called as tar or bio-oil. When steam reforming reaction of the tar can proceed at low temperature comparable to the case of the pyrolysis, the combination of the rapid pyrolysis and catalytic steam reforming will enable the low-temperature gasification of biomass to synthesis gas and hydrogen.

In the steam reforming of tar, catalysts with high performance in terms of the activity and stability are needed. Moreover, it is considered that high abilities in the catalyst activation and the catalyst regeneration are important properties in the process for the biomass conversion to synthesis gas and hydrogen. If the catalysts can be activated automatically by the introduction of the biomass tar at the reaction temperature, this self-activation property can contribute to the easier operation of the process. On the other hand, the coke deposited on the catalysts can be reduced to some extent, but the complete suppression is difficult. The coke removal such as by the combustion is necessary. However, the procedure for the coke removal can cause the catalyst deactivation by the sintering of a support material and the aggregation of metal particles. If the catalysts are recyclable by the re-dispersion of the aggregated particles, the catalyst cost can be decreased. The self-activation and self-regeneration properties as well as high steam reforming activity and the suppression of coke formation can contribute to the development of more feasible process. Applicability of the commercial and conventional steam reforming catalysts has been evaluated [5–10]. However, in fact, the performance of the conventional catalysts is not satisfactory, and the development of the catalysts for the steam reforming of tar derived from the biomass pyrolysis is highly needed.

Table 1 lists the examples of recent reports on Ni catalysts for the tar conversion in the gasification of real biomass. A nano-NiO/γ-Al_2O_3 catalyst was reported by Li et al. [11] to show high activity in cracking of tar and hydrocarbons. Another nano-Ni-La-Fe/Al_2O_3 catalyst was also developed by Li et al. [12]. In the presence of the catalyst, the tar remove efficiency reached 99% at 1073 K, and the coke deposition and sintering effects were avoided, leading to a

Table 1 Recent reports on Ni catalysts for biomass gasification

Biomass	Catalyst	Ni content (wt%)	Catalyst amount (g)	Reactor (diameter × height, mm)	Ref.
Rice husk	$NiO/\gamma\text{-}Al_2O_3$	12	1000	fixed-bed (88 × 1200)	[11]
Sawdust	$NiO/\gamma\text{-}Al_2O_3$	12	1000	fixed-bed (88 × 1200)	[12]
Sawdust	$Ni\text{-}La\text{-}Fe/\gamma\text{-}Al_2O_3$	8.6	1000	fixed-bed (88 × 1200)	[12]
Pine sawdust	NiO-MgO	19.5	20	fluidized-bed (20 × 800)	[13]
Pine sawdust	Ni/MgO	19.5	20	fluidized-bed (20 × 800)	[13]
Pine sawdust	$Ni_{0.03}Mg_{0.97}O$	4.3	20	fluidized-bed (20 × 800)	[13]
Red pine	Ni/Al_2O_3	20	45	fixed-bed (53.5 × 610)	[14]
Red pine	Ni/Al_2O_3	20	100	fixed-bed (53.5 × 610)	[15]
Red pine	Ni/coal char	9	100	fixed-bed (53.5 × 610)	[14,15]
Sawdust	Ni/wood char	5–20	18	fixed-bed (25 × 610)	[16]
Sawdust	Ni/coal char	5–20	18	fixed-bed (25 × 610)	[16]
Eucalyptus twig sawdust	NiO/dolomite	0.4–4.3	2	fixed-bed (22 × 700)	[17]
Cedar	Ni/oxide (oxide: Al_2O_3, ZrO_2, TiO_2, CeO_2, MgO)	12	1	fixed-bed (10 × 290)	[26]
Cedar	$Ni/CeO_2/Al_2O_3$	4, 12	1	fixed-bed (10 × 290)	[27,28]
Cedar	$M\text{-}Ni/CeO_2/Al_2O_3$ (M = Pt, Pd, Rh, Ru)	4, 12	1	fixed-bed (10 × 290)	[29,30]
Cedar	$Pt/Ni/CeO_2/MgO/Al_2O_3$	12	1	fixed-bed (10 × 290)	[31]
Cedar	$Ni/MnO/Al_2O_3$	12	1	fixed-bed (10 × 290)	[32]

long lifetime of catalysts. Wang et al. [13] reported a NiO-MgO catalyst exhibiting high stable activity for the reforming of raw fuel gas from gasifier. The highly stable activity was attributed to the high dispersion of Ni particles in the NiO-MgO solid solution structure and the promotion by catalyst reducibility. Recently, Le et al. [14] developed a Ni-loaded brown coal char for the steam reforming of tar. Compared to conventional Ni/Al_2O_3, Ni-loaded brown coal char has a higher activity and stability with coke resistance [15]. It was also reported by Wang et al. [16] that coal char supported Ni and wool char supported Ni catalysts are effective for tar removal, converting more than 97% of tars in synthesis gas at 1073 K. Corujo et al. [17] reported that the use of NiO-loaded calcined dolomite catalysts led to a reduction in the formation rate of tar and char and a 30% increase in the total product gas. As listed in Table 1, the amount of catalysts was rather large in most cases. This large amount of catalysts needed for the activity tests makes it difficult to optimize the catalyst composition, the preparation method, pre-treatment conditions, and so on. In fact, the number of the tested catalysts in most cases is so limited. On the other hand, in our case, the reactor size is rather small, and only 1 g catalyst is needed, then various catalysts can be easily tested and this enables the development of the catalysts tuned for the catalytic gasification of biomass [18–25] and the steam reforming of the biomass tar [26–34].

On the other hand, addition of secondary metal or metal oxide is a promising approach for tuning or design new catalysts. In this approach, the optimum amount of the additives is usually present. For example, in the case of metal catalysts modified with oxides and secondary metals, the interface between metal and the modifier can be a catalytically active site, and the amount of the interface has a maximum with respect to the additive amount of the modifier, such as Rh-M/MgO (M = Co, Ni, Fe) catalysts for the catalytic partial oxidation of methane [35–37], Rh-MO_x (M = Mo, Re) catalysts for the hydrogenolysis of biomass-derived polyols and cyclic ethers [38–42], Pt-ReO_x catalysts for the preferential CO oxidation in a H_2-rich stream [43,44], and so on. It has been known that Ni is one of the suitable components for the steam reforming of various organic compounds, and the effects of supports and additive oxides and other metals have been investigated. Our group has reported that the addition of CeO_2 [27,28] and MnO [32] to Ni catalysts enhanced the catalytic performance in terms of the activity and the suppression of coke formation in the steam reforming of the biomass tar. In particular, the suppression of coke formation is related to the catalyst stability. We also attempted to attach the self-activation and self-regeneration properties to $Ni/CeO_2/Al_2O_3$ catalysts by modification with a small amount of Pt and MgO [29–31].

This review article shows the development process of Ni/Al_2O_3 modified with CeO_2, Pt, and MgO in order to make the multi-functional catalyst for the steam reforming of tar derived from the wood pyrolysis.

1 Steam reforming of tar over Ni catalysts supported on different oxides [26]

Ni catalysts supported on various oxides, i.e., Ni/Al_2O_3, Ni/ZrO_2, Ni/TiO_2, Ni/CeO_2, and Ni/MgO were prepared by the incipient wetness method using an aqueous solution of $Ni(NO_3)_2{\cdot}6H_2O$. The method for the preparation of the sup-

port materials were described in our previous report [26]. The calcination conditions for the preparation of the supports are listed in Table 2. It should be noted that all the alumina supports in this review were α-Al_2O_3. After impregnation, the sample was dried at 383 K for 12 h followed by calcination at 773 K for 3 h under air atmosphere. The loading amount of Ni is described in parentheses as mass percent on all the catalysts. Cedar wood was used as the biomass feedstock for all experiments. Steam reforming of tar was carried out in a laboratory-scale continuous feeding dual-bed reactor [26]. In this system, tar is formed by the rapid pyrolysis of cedar wood in the presence of steam, and it is introduced to the secondary catalyst bed together with steam. Before catalytic reaction, the catalyst was pre-reduced in H_2 at 773 K for 0.5 h.

Table 2 Properties of Ni catalysts supported on different oxides [26]

Catalyst	Calcination conditions		BET surface area	H_2 adsorption[b]	Reduction degree	Dispersion[d]	Particle size of Ni metal (nm)	
	Temperature (K)	Time (h)	(m^2/g_{cat})	(10^{-6} mol/g_{cat})	from TPR[c] (%)	(%)	H_2 adsorption[e]	XRD[f]
Ni(12)/Al_2O_3	1423	1	8	27	106	2.7	36	31
Ni(12)/ZrO_2	1073	3	10	30	96	3.0	31	29
Ni(12)/TiO_2	1173	3	16	28	97	2.8	34	21
Ni(12)/CeO_2	1073	3	12	17	106	1.7	56	58
Ni(12)/MgO	—[a]	—	12	3	20	1.5	64	n.d.

[a]MgO support was used without precalcination.

[b]H_2 adsorption is total adsorption at room temperature, and H/Ni = 1 is assumed.

[c]Calculated by (H_2 consumption in TPR profiles)/(loading amount of Ni) × 100%, assuming that $Ni^{2+} + H_2 \rightarrow Ni^0 + 2H^+$.

[d]Dispersion calculated by 2 × (H_2 adsorption)/(loading amount of Ni)/(reduction degree) × 100% [45,46].

[e]Particle size of Ni metal calculated by the relation: (particle size/nm) = 9.71/(dispersion/%) × 10 [45,46].

[f]Particle size of Ni metal calculated from the Scherrer equation, using the full width at half height of the strong intensity metal peak.

Table 3 summarizes the results of various supported Ni catalysts in steam reforming of tar at 823 K together with that in the absence of catalyst. Without catalyst, the tar yield was rather high and the formation rates of CO and H_2 were quite low. On the other hand, when Ni catalysts were used, the yield of tar decreased and the formation rate of gaseous products, especially H_2, increased drastically compared to the case of no catalyst. This result indicates that Ni catalysts are effective for the conversion of tar to useful gases such as CO and hydrogen. It should be noted that the catalytic performance was strongly dependent on support materials.

Table 3 Catalyst performance in steam reforming of tar derived from the pyrolysis of cedar wood over various oxide supported Ni catalysts at 823 K [26]

Catalyst	Formation rate (μmol/min)					H_2/CO	C-conversion	Char (%)	Coke (%)	Tar (%)
	CO	H_2	CH_4	C_2	CO_2	ratio	(%)			
Ni(12)/Al_2O_3	706	938	157	48	420	1.3	59	19	12.7	9.3
Ni(12)/ZrO_2	615	1222	95	17	559	2.0	59	22	6.6	12.4
Ni(12)/TiO_2	624	950	142	31	411	1.5	53	19	15.1	12.9
Ni(12)/CeO_2	565	781	121	40	349	1.4	50	20	4.3	25.7
Ni(12)/MgO	569	417	142	36	251	0.7	45	16	10.4	28.6
No catalyst	603	269	132	66	189	0.4	45	24	0.0	31.0

Reaction conditions: biomass 60 mg/min (H_2O, 9.2%; C, 2320 μmol/min; H, 3220 μmol/min; O, 1430 μmol/min), H_2O/C = 0.5, catalyst 1.0 g, H_2 reduction at 773 K for 30 min.

Figure 1(a) compares the yields of the residual tar and coke in steam reforming of tar at 823 K over various Ni catalysts. In terms of the residual tar yield, the order of the activity at 823 K was as follows: Ni/Al_2O_3 > Ni/ZrO_2 > Ni/TiO_2 > Ni/CeO_2 > Ni/MgO > no catalyst. The amount of H_2 adsorption listed in Table 2 explains the order of the steam reforming activity. Low activity of Ni/MgO is also affected by low reduction degree of Ni species. On the other hand, the coke yield was in the order: Ni/TiO_2 > Ni/Al_2O_3 > Ni/MgO > Ni/ZrO_2 > Ni/CeO_2, which cannot be explained by the amount of H_2 adsorption, and this suggests that the function of the support oxide is very important. The tar and coke yields on various Ni catalysts are plotted in Fig. 1(d). The coke deposited on the catalyst can be formed by the decomposition of tar and the disproportionation of CO as a product of steam reforming. When the coke yield increases with decreasing the tar yield, it is thought that the coke is mainly formed by the decomposition of tar. However, in

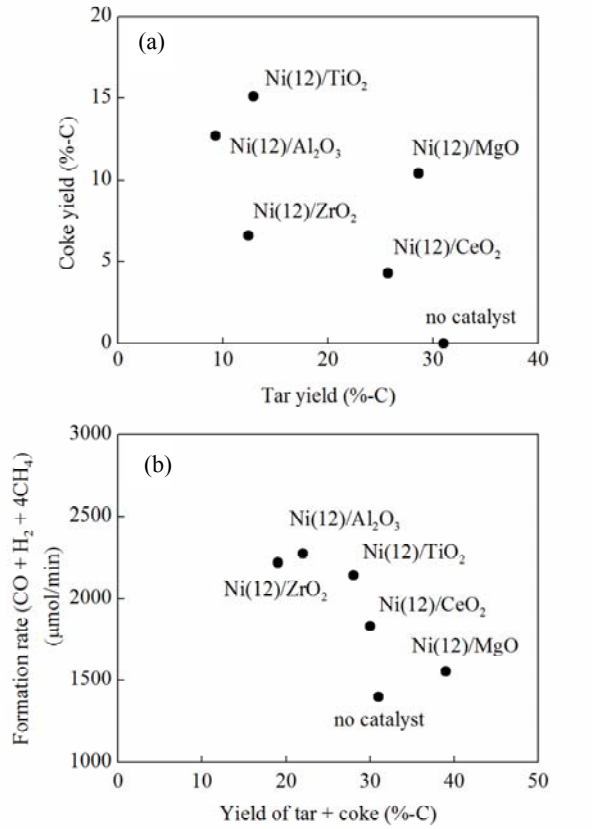

Fig. 1. Formation of tar and coke in steam reforming of tar over various Ni catalysts (a) and the relation between the yields of tar + coke and formation rate of CO + H_2 + 4CH_4 over various Ni catalysts (b) [26]. Reaction conditions: biomass 60 mg/min (H_2O, 9.2%; C, 2320 μmol/min; H, 3220 μmol/min; O, 1430 μmol/min), steam 1110 μmol/min, H_2O/C = 0.5, 823 K, 15 min, catalyst 1.0 g, H_2 reduction at 773 K for 30 min.

fact, the relation between tar and coke yields was complex, suggesting that the coke is also formed by the CO disproportionation. In contrast, the relation between the formation rate of CO + H_2 + 4CH_4 and the yield of tar + coke (Fig. 1(b)) is clear, and low yield of tar + coke is connected to higher formation rate of the combustible gases. It is concluded that the catalyst with high steam reforming activity and the suppression of coke formation is directly connected to the efficient production of synthesis gas.

Figure 2 shows the TPR profiles of various Ni catalysts. The reduction degree estimated from the results of H_2 consumption in TPR profiles is listed in Table 2. Except for Ni/MgO, the reduction degree of Ni was almost 100% and this indicates that all the Ni was reduced at about 800 K. On the other hand, the reduction degree of Ni/MgO was only about 20%. This can be because the strong interaction between NiO and MgO decreases catalyst reducibility [47–49]. An important point is that the reduction profile of Ni is strongly influenced by the support oxides, and Ni species on CeO_2 showed high reducibility. The similar behavior

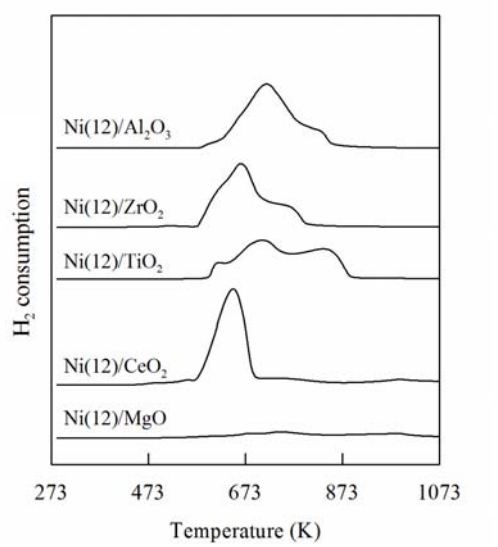

Fig. 2. TPR profiles of various Ni catalysts [26]. Conditions: heating rate, 10 K/min; room temperature to 973 K, and the temperature was maintained at 973 K for 30 min; 5% H_2/Ar, flow rate 30 ml/min.

was also observed in the case of Rh-CeO_2 catalysts [50].

To investigate the catalyst ability for coke removal, we measured the reactivity of coke with catalysts using active carbon as a model compound of coke by means of thermogravimetric analysis (TGA). Figure 3 shows the TGA profiles of active carbon + catalyst in 5% steam/N_2. Compared to no catalyst, the presence of catalysts promoted steam gasification of active carbon. In particular, Ni/CeO_2 was more effective than the other catalysts. The promotion of reaction between steam and active carbon can cause low coke yield in steam reforming of tar over Ni/CeO_2. This property is due to high redox property of Ce species, and reduction and oxidation of Ce species proceed in the presence of steam and tar [50].

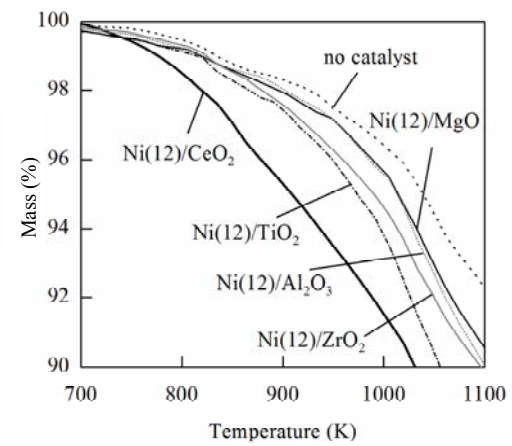

Fig. 3. TGA profiles of active carbon mixed with catalysts under air atmosphere [26]. Conditions: sample, 5 mg active carbon + 5 mg catalyst; heating rate, 15 K/min, room temperature to 1273 K; air flow rate, 20 ml/min.

2 Steam reforming of tar over $Ni/CeO_2/Al_2O_3$ catalysts [27,28]

As mentioned above, the interaction of Ni and CeO_2 gave high reducibility of Ni species and the suppression of coke formation. Therefore, the additive effect of CeO_2 to Ni/Al_2O_3 was investigated, and in particular, the relation between the Ni-CeO_2 interaction and catalytic performance in the steam reforming of tar was clarified. Two types of $Ni/CeO_2/Al_2O_3$ catalysts were prepared by the co-impregnation (CI) and sequential impregnation (SI) methods [27,28]. Here, different preparation methods were attempted in order to control the interaction between Ni and CeO_2. In co-impregnation, the Al_2O_3 was impregnated with an aqueous solution of $Ni(NO_3)_2{\cdot}6H_2O$ and $Ce(NH_4)_2(NO_3)_6$, followed by drying and calcination at 773 K for 3 h. In sequential impregnation, the Al_2O_3 was impregnated with $Ce(NH_4)_2(NO_3)_6$ solution, followed by drying and calcination at 773 K for 3 h, and then impregnated with $Ni(NO_3)_2{\cdot}6H_2O$ solution, followed by drying and calcination at 773 K for 3 h. The loading amounts of Ni and CeO_2 are described in parentheses as mass percent on all the catalysts.

Figure 4 shows the catalytic performances of $Ni/CeO_2/Al_2O_3$ catalysts in steam reforming of tar at 823 K. On 4 wt% Ni catalysts, $Ni(4)/CeO_2(30)/Al_2O_3$ (CI) exhibited higher activity than $Ni(4)/Al_2O_3$ and $Ni(4)/CeO_2(30)/Al_2O_3$ (SI) catalysts, and at the same time, $Ni(4)/CeO_2(30)/Al_2O_3$ (CI) also showed higher resistance to coke formation. Similar tendency was also observed on 12 wt% Ni catalysts. These results demonstrate that the co-impregnation is an effective preparation method for $Ni/CeO_2/Al_2O_3$.

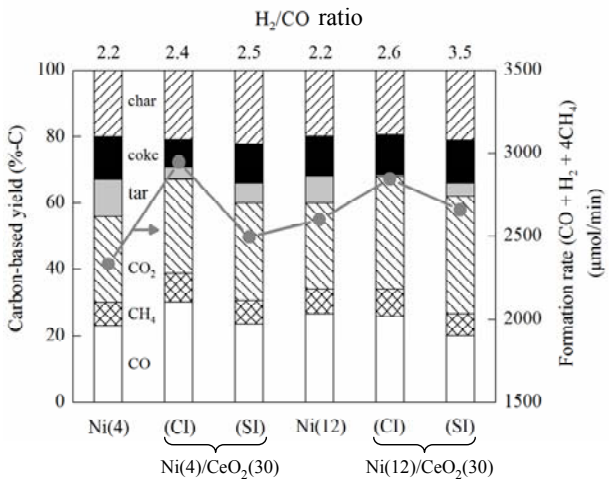

Fig. 4. Catalytic performances of $Ni/CeO_2/Al_2O_3$ in steam reforming of tar [27,28]. Conditions: biomass, 60 mg/min (H_2O, 10.4%; C, 2191 μmol/min; H, 3543 μmol/min; O, 1478 μmol/min); steam, 1110 μmol/min, (added H_2O)/C = 0.5; reaction temperature, 823 K; reaction time, 15 min; catalyst, 1.0 g; H_2 reduction at 773 K for 30 min. Loading amount: Ni, 4 and 12 wt%; CeO_2, 30 wt%.

Figure 5 shows TPR profiles of Ni/Al_2O_3 and $Ni/CeO_2/Al_2O_3$ catalysts. On $Ni(4)/Al_2O_3$, the H_2 consumption was observed in the temperature range between 630 and 850 K. In the presence of CeO_2, the peak of H_2 consumption was shifted to lower temperature. The shift on $Ni(4)/CeO_2(30)/Al_2O_3$ (CI) was more significant than that on $Ni(4)/CeO_2(30)/Al_2O_3$ (SI). A similar phenomenon was also observed on the 12 wt% Ni catalysts. The lower temperature shift of H_2 consumption peak by the addition of CeO_2 can be explained by the interaction between Ni species and CeO_2. The larger shift on $Ni/CeO_2/Al_2O_3$ (CI) than that on $Ni/CeO_2/Al_2O_3$ (SI) can be interpreted by the stronger interaction between Ni and CeO_2 introduced by the co-impregnation method. Another important point is that the Ni-based reduction degree on the CI catalysts is higher than that on the SI catalysts, and especially, the reduction degree of $Ni(4)/CeO_2(30)/Al_2O_3$ (CI) was high (Table 4).

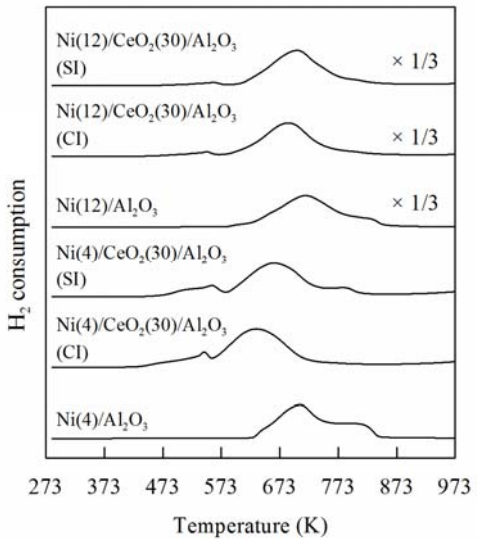

Fig. 5. TPR profiles of $Ni/CeO_2/Al_2O_3$ catalysts [27,28]. Conditions: heating rate, 10 K/min; room temperature to 973 K, and the temperature was maintained at 973 K for 10 min; 5% H_2/Ar, 30 ml/min; sample amount, 50 mg.

Assuming that the CeO_2 around Ni can be reduced more easily, these results also support the stronger interaction between Ni and CeO_2 on $Ni(4)/CeO_2(30)/Al_2O_3$ (CI). The characterization by TEM and EXAFS analysis showed that the particle size of Ni over $Ni(4)/CeO_2(30)/Al_2O_3$ (CI) was smaller than those over $Ni(4)/Al_2O_3$ and $Ni(4)/CeO_2(30)/Al_2O_3$ (SI) [28]. Nevertheless, the amount of H_2 adsorption on $Ni(4)/CeO_2(30)/Al_2O_3$ (CI) was a little smaller than those on the other two catalysts (Table 4). The inconsistence between the results of TEM and EXAFS and that of H_2 adsorption can be explained by covering Ni with CeO_2 over $Ni(4)/CeO_2(30)/Al_2O_3$ (CI), which also supports that the strong interaction between Ni and CeO_2 can be realized by

Table 4 Physicochemical properties of $Ni/CeO_2/Al_2O_3$ catalysts [27,28]

Catalyst	BET surface area (m^2/g_{cat})	H_2 consumption[a] (10^{-3} mol/g_{cat})	H_2/Ni[b]	H_2 adsorption[c] (H/Ni)
$Ni(4)/Al_2O_3$	9	0.71	1.04	0.045
$Ni(4)/CeO_2(30)/Al_2O_3$ (CI)	30	1.01	1.56	0.031
$Ni(4)/CeO_2(30)/Al_2O_3$ (SI)	13	0.95	1.39	0.042
$Ni(12)/Al_2O_3$	13	2.11	1.03	0.030
$Ni(12)/CeO_2(30)/Al_2O_3$ (CI)	22	2.36	1.15	0.021
$Ni(12)/CeO_2(30)/Al_2O_3$ (SI)	13	2.26	1.10	0.019

[a]H_2 consumption below 773 K in TPR profiles.

[b]Calculated by (H_2 consumption)/(loading amount of Ni), assuming that $Ni^{2+} + H_2 \rightarrow Ni^0 + 2H^+$.

[c]H_2 adsorption is total adsorption at room temperature, and H/Ni = 1 is assumed.

the co-impregnation method. According to the catalyst characterization, the particle size of Ni metal and CeO_2 was about 7 and 8 nm, respectively [28], and the TEM image suggests that 100 nm Ni-CeO_2 nanocomposite consisted of 7–8 nm Ni metal and CeO_2 particles. The formation of nanocomposite enables large interface of Ni-CeO_2. This property can be related to the excellent performance in steam reforming of tar. It is suggested that CeO_2 can supply oxygen atom to the adsorbed species on Ni metal surface at the interface. The carbonaceous reaction intermediate species adsorbed on Ni metal surface can react with oxygen atom supplied from neighboring CeO_2, resulting in high catalytic activity and low coke formation. The role of the interface between Ni and CeO_2 is illustrated in Fig. 6.

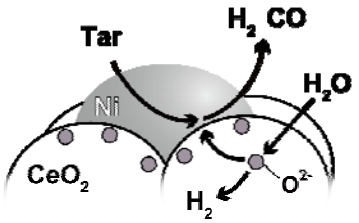

Fig. 6. Role of the Ni-CeO_2 interface on Ni-CeO_2 nanocomposite in steam reforming of tar.

3 Steam reforming of tar over $Ni/CeO_2/Al_2O_3$ modified with noble metals [29,30]

It has been reported that the modification of Ni catalysts for steam reforming of hydrocarbons with a small amount of noble metals enhances the catalytic performance remarkably from the aspects of activity, suppression of coke formation, catalyst reducibility, catalyst activation, and so on [51–62]. Pt, Pd, Rh, and Ru were loaded on $Ni(4)/CeO_2(30)/Al_2O_3$ (CI) using an aqueous solution of $Pt(NO_2)_2(NH_3)_2$, $Pd(NO_3)_2$, $Rh(NO_3)_3$, and $Ru(NO)(NO_3)_3$, respectively [29,30]. After impregnation, the sample was dried, followed by calcination at 773 K for 3 h. The loading amount of each component is described in parentheses as mass percent on all the catalysts.

Figure 7 shows the catalytic performances of noble metal-modified $Ni(4)/CeO_2(30)/Al_2O_3$ catalysts in steam reforming of tar at 823 K. Here, the catalysts without H_2 reduction were compared in order to evaluate the effect of noble metals on the self-activation. The modification by noble metals improved the catalytic activity. Among noble metals investigated, Pt was the most effective. On $Pt(0.1)/Ni(4)/CeO_2(30)/Al_2O_3$, the tar yield was almost zero. This performance is higher than that of $Ni(4)/CeO_2(30)/Al_2O_3$ with reduction pretreatment (Fig. 4). The promoting effect of Pt was so significant that the addition of a very small amount of Pt such as 0.01 wt% to the $Ni(4)/CeO_2(30)/Al_2O_3$ catalyst also enhanced the performance drastically. We have verified that $Pt(0.1)/CeO_2(30)/Al_2O_3$ showed much lower performance than $Ni(4)/CeO_2(30)/Al_2O_3$ and $Pt(0.1)/Ni(4)/CeO_2(30)/Al_2O_3$ [30]. Therefore, the activity of $Pt/Ni(4)/CeO_2(30)/Al_2O_3$ was mainly due to Ni species and the addition of Pt enhanced the activity of Ni species.

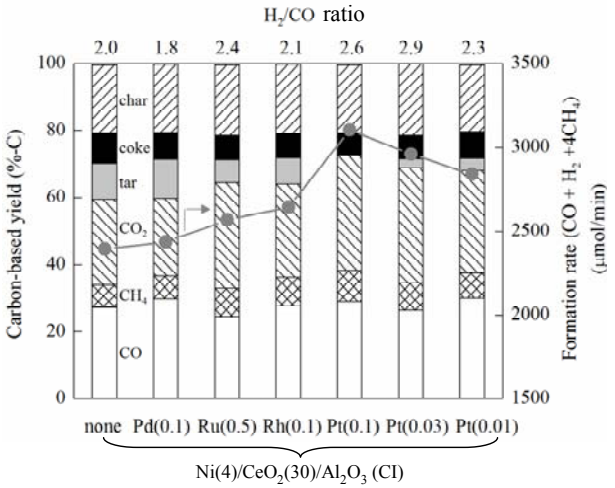

Fig. 7. Catalytic performance in steam reforming of tar over noble metal-modified $Ni(4)/CeO_2(30)/Al_2O_3$ (CI) [30]. Reaction conditions: biomass, 60 mg/min (H_2O 9.2%; C, 2191 μmol/min; H, 3543 μmol/min; O, 1475 μmol/min); steam, 1110 μmol/min, (added H_2O)/C = 0.5; reaction temperature, 823 K; reaction time, 15 min; catalyst, 1.0 g; without reduction. Loading amount: Ni, 4 wt%; CeO_2, 30 wt%; Pd, 0.1 wt%; Ru, 0.5 wt%; Rh, 0.1 wt%; Pt, 0.01–0.1 wt%.

Figure 8 shows the TPR profiles of $Ni(4)/CeO_2(30)/Al_2O_3$ modified with noble metals. The addition of 0.1 wt% Pt increased hydrogen consumption at 520 K and decreased that at 620 K. On the other hand, no peaks were observed on $Pt(0.1)/CeO_2(30)/Al_2O_3$ around 520 K. These indicate that the peak at 520 K on $Pt(0.1)/Ni(4)/CeO_2(30)/Al_2O_3$ can be assigned to the reduction of NiO promoted by the Pt addition. From the comparison between the TPR profiles of

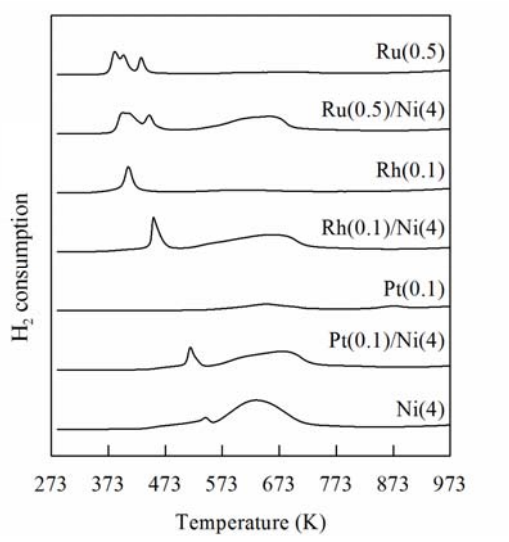

Fig. 8. TPR profiles of noble metal-modified Ni(4)/CeO_2(30)/Al_2O_3 (CI) [30]. Conditions: heating rate 10 K/min, room temperature to 973 K; 5% H_2/Ar, 30 ml/min; sample amount, 50 mg. Loading amount: Ni, 4 wt%; Pt, 0.1 wt%; Rh, 0.1 wt%; Ru, 0.5 wt%.

M/Ni/CeO_2/Al_2O_3 and M/CeO_2/Al_2O_3 (M = Rh and Ru), the lower temperature peaks below 500 K may be assigned to the reduction of CeO_2 promoted by the presence of Rh and Ru, and these behaviors are different from the case of Pt. These results suggest that Pt tends to interact with NiO species, and other noble metals tend to interact with CeO_2. This was supported by EXAFS results that Pt-Ni alloy was formed [30], while Rh, Ru, and Pd did not alloy with Ni. Combination of catalytic performance and characterization results suggests that high performance of Pt/Ni/CeO_2/Al_2O_3 can be due to the strong interaction between Pt and Ni to form Pt-Ni alloy.

In addition, the coke was formed on Pt/Ni/CeO_2/Al_2O_3 during the reaction as shown in Fig. 7, and this can deactivate the catalyst. The deposited coke was removed by the combustion with air, but one problem is the aggregation of Ni metal particles during the reaction and regeneration procedure [31]. Therefore, the re-dispersion of Ni metal particles by the catalyst regeneration is thought to be necessary. It has been known that the interaction of Ni and MgO is strong and NiO-MgO solid solution is easily formed. At the same time, the reduction of the NiO-MgO solid solution gives small Ni metal particles [48,62,63]. We expect that the re-dispersion of aggregated Ni metal particles can be attached by the addition of MgO to the catalyst via formation and reduction of NiO-MgO solid solution.

4 Steam reforming of tar over Pt/Ni/CeO_2/MgO/Al_2O_3 [31]

Ni/CeO_2/MgO/Al_2O_3 (CI) was prepared by the co-impregnation method using an aqueous solution of $Ni(NO_3)_2 \cdot 6H_2O$, $Ce(NH_4)_2(NO_3)_6$, and $Mg(NO_3)_2 \cdot 6H_2O$ [31] in a similar way for Ni/CeO_2/Al_2O_3 (CI). Pt/Ni/CeO_2/MgO/Al_2O_3 (CI) was prepared by the impregnation of aqueous solution of $Pt(NO_2)_2(NH_3)_2$ on Ni/CeO_2/MgO/Al_2O_3 (CI) in the same way for Pt/Ni/CeO_2/Al_2O_3 (CI). As a reference, Pt/Ni/MgO/Al_2O_3 (CI) was prepared in a similar way. The loading amount of each component is described in parentheses as mass percent on all the catalysts. Figure 9 shows the catalytic performance of Pt(0.1)/Ni(12)/CeO_2(15)/MgO(2)/Al_2O_3 together with those of Pt(0.1)/Ni(12)/CeO_2(15)/Al_2O_3 and Pt(0.1)/Ni(12)/MgO(2)/Al_2O_3.

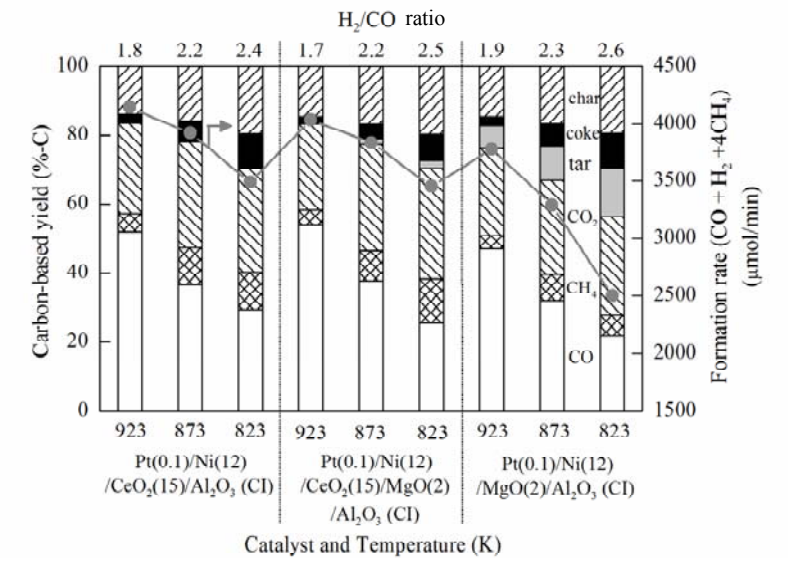

Fig. 9. Catalytic performance in steam reforming of tar on Pt(0.1)/Ni(12)/CeO_2(15)/Al_2O_3, Pt(0.1)/Ni(12)/CeO_2(15)/MgO(2)/Al_2O_3, and Pt(0.1)/Ni(12)/MgO(2)/Al_2O_3 [31]. Conditions: biomass, 60 mg/min (H_2O, 9.2%; C, 2191 μmol/min; H, 3543 μmol/min; O, 1475 μmol/min); steam, 1110 μmol/min, (added H_2O)/C = 0.5; reaction time, 15 min; catalyst, 1.0 g; H_2 reduction at 773 K for 30 min.

Judging from the tar yield, the order of the catalytic activity is as follows: Pt(0.1)/Ni(12)/CeO_2(15)/Al_2O_3 ≈ Pt(0.1)/Ni(12)/CeO_2(15)/MgO(2)/Al_2O_3 >> Pt(0.1)/Ni(12)/MgO(2)/Al_2O_3. It should be noted that the addition of MgO to Pt(0.1)/Ni(12)/CeO_2(2)/Al_2O_3 suppressed the carbon formation to some extent. Although the details are not shown here, Ni(12)/CeO_2(15)/MgO(2)/Al_2O_3 showed lower activity than Ni(12)/MgO(2)/Al_2O_3. However, it is found that the performance of Pt(0.1)/Ni(12)/CeO_2(15)/MgO(2)/Al_2O_3 became comparable to that of Pt(0.1)/Ni(12)/CeO_2(15)/Al_2O_3 in the presence of a small amount of added Pt.

Figure 10 displays the formation rate of the gaseous products with time on stream over Pt(0.1)/Ni(12)/CeO_2(15)/MgO(2)/Al_2O_3 without H_2 reduction pretreatment. The formation rate increased with time on stream and it reached the similar value to that over the catalyst with H_2 reduction pretreatment after 12 min. This result indicates that the tar derived from the pyrolysis of cedar wood can reduce the catalyst, although the reduction of Pt(0.1)/Ni(12)/CeO_2(15)/MgO(2)/Al_2O_3 was not so rapid as described below. This behavior indicates that the Pt(0.1)/Ni(12)/CeO_2(15)/MgO(2)/Al_2O_3 catalyst can be activated automatically by the reactants, which is regarded as the ability of the self-activation property [57,60–62].

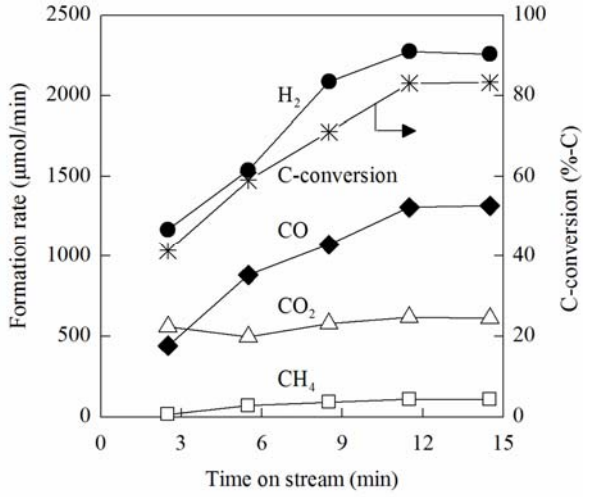

Fig. 10. Catalytic performance with time on stream over Pt(0.1)/Ni(12)/CeO_2(15)/MgO(2)/Al_2O_3 (CI) without H_2 reduction [31]. Reaction conditions: biomass, 60 mg/min (H_2O, 9.2%; C, 2191 μmol/min; H, 3543 μmol/min; O, 1475 μmol/min); steam, 1110 μmol/min, (added H_2O)/C = 0.5; reaction temperature, 923 K; catalyst, 1.0 g.

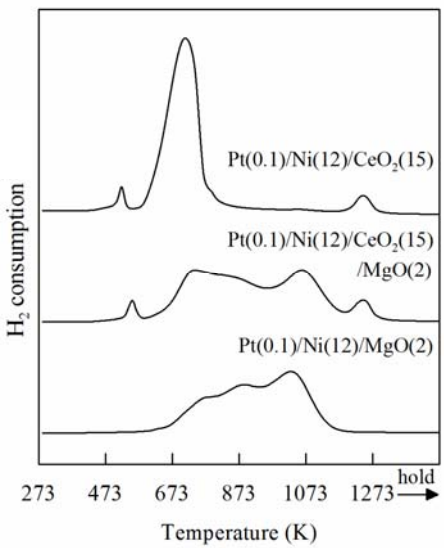

Fig. 11. TPR profiles of Pt(0.1)/Ni(12)/CeO_2(15)/MgO(2)/Al_2O_3, Pt(0.1)/Ni(12)/CeO_2(15)/Al_2O_3, and Pt(0.1)/Ni(12)/MgO(2)/Al_2O_3 catalysts [31]. Conditions: heating rate, 10 K/min; room temperature to 1273 K, and the temperature was maintained at 1273 K for 30 min; 5% H_2/Ar, 30 ml/min; sample amount, 200 mg.

Figure 11 shows the TPR profiles of the calcined catalysts. The amount of H_2 consumption below 773 K and the Ni-based reduction degree estimated from the amount of H_2 consumption are listed in Table 5. On Pt(0.1)/Ni(12)/CeO_2(15)/Al_2O_3, the reduction proceeds mainly below 773 K. The profile of Pt(0.1)/Ni(12)/CeO_2(15)/MgO(2)/Al_2O_3 was greatly different from that of Pt(0.1)/Ni(12)/CeO_2(15)/Al_2O_3, and this can be explained by the effect of the presence of MgO. On Pt(0.1)/Ni(12)/CeO_2(15)/MgO(2)/Al_2O_3,

Table 5 Physicochemical properties of Pt/Ni/CeO_2/Al_2O_3, Pt/Ni/CeO_2/MgO/Al_2O_3, and Pt/Ni/MgO/Al_2O_3 catalysts after H_2 reduction at 773 K [31]

Catalyst	BET surface area (m^2/g_{cat})	H_2 consumption[a] (10^{-3} mol/g_{cat})	Ni-based reduction degree[b] (%)	H_2 adsorption[c] (10^{-6} mol/g_{cat})	Dispersion[d] (%)	Particle size of Ni metal[e] (nm)
Pt(0.1)/Ni(12)/CeO_2(15)/Al_2O_3 (CI)	18.8	1.51	96	4.2	5.6	17.5
Pt(0.1)/Ni(12)/CeO_2(15)/MgO(2)/Al_2O_3 (CI)	19.2	0.47	30	3.9	16.6	5.9
Pt(0.1)/Ni(12)/MgO(2)/Al_2O_3 (CI)	9.1	0.24	15	2.4	20.0	4.9

[a]H_2 consumption below 773 K in TPR profiles.

[b]Calculated by (H_2 consumption)/(loading amount of Ni) × 100%, assuming that $Ni^{2+} + H_2 \rightarrow Ni^0 + 2H^+$ and that the reduction of Pt and CeO_2 was neglected.

[c]H_2 adsorption is total adsorption at room temperature, and H/Ni = 1 is assumed. The adsorption of H_2 on Pt was neglected because of the small molar ratio of Pt to Ni.

[d]Dispersion calculated by 2 × (H_2 adsorption)/(loading amount of Ni)/(reduction degree) × 100% [45,46].

[e]Particle size of Ni metal calculated by the relation: particle size (nm) = 9.71/dispersion (%)× 10 [45,46].

the temperature range of the H_2 consumption was much broader. The TPR profile of Pt(0.1)/Ni(12)/MgO(2)/Al_2O_3 was also obtained, and the main peak was located at about 1073 K. As shown in Fig. 2, the NiO on α-Al_2O_3 can be reduced below 873 K. Based on these results, it is interpreted that the presence of MgO decreases the reducibility of Ni species and it can be caused by the strong interaction between NiO and MgO obtained by the formation of NiO-MgO solid solution. The molar ratio of MgO to NiO is only 1/4, but the effect of MgO is rather strong. The Ni-based reduction degree on Pt(0.1)/Ni(12)/CeO_2(15)/Al_2O_3 below 773 K decreased significantly to about 1/3 by the addition of MgO. This tendency was more remarkable on Pt(0.1)/Ni(12)/MgO(2)/Al_2O_3. In addition, the amount of H_2 adsorption on fresh catalysts is also listed in Table 5. The amount of H_2 adsorption on Pt(0.1)/Ni(12)/CeO_2(15)/MgO(2)/Al_2O_3 was almost the same as that on Pt(0.1)/Ni(12)/CeO_2(15)/Al_2O_3, although the reduction degree was much lower. This behavior indicates that the MgO addition promotes the dispersion of Ni metal particles, although it decreases the reduction degree of Ni species. The negative effect can be compensated by the promoting effect. The amount of H_2 adsorption on Pt(0.1)/Ni(12)/MgO(2)/Al_2O_3 was much smaller than those on other catalysts, and this can be connected to lower catalytic performance in the steam reforming of tar (Fig. 9). Furthermore, the TPR profile of Pt(0.1)/Ni(12)/CeO_2(15)/MgO(2)/Al_2O_3 is also related to the performance of catalysts without H_2 reduction (Fig. 10). The slower activation process by the tar over Pt(0.1)/Ni(12)/CeO_2(15)/MgO(2)/Al_2O_3 is explained by the lower reducibility.

Figure 12 shows the catalytic performance with time on stream at 923 K over the Pt(0.1)/Ni(12)/CeO_2(15)/Al_2O_3 and Pt(0.1)/Ni(12)/CeO_2(15)/MgO(2)/Al_2O_3 catalysts. The formation rate and C-conversion on the Pt(0.1)/Ni(12)/CeO_2(15)/Al_2O_3 catalyst decreased drastically at about 120 min, and this behavior corresponded to catalyst deactivation [31]. On the other hand, the Pt(0.1)/Ni(12)/CeO_2(15)/MgO(2)/Al_2O_3 catalyst maintained high activity even after 240 min. This indicated that the addition of MgO can improve the catalyst stability.

The dispersion of the Pt(0.1)/Ni(12)/CeO_2(15)/MgO(2)/Al_2O_3 is higher than that of Pt(0.1)/Ni(12)/CeO_2(15)/Al_2O_3 (Table 5) and MgO addition enhanced the Ni dispersion caused by strong interaction between Ni and MgO. Figure 13 shows the XRD patterns of Pt(0.1)/Ni(12)/CeO_2(15)/Al_2O_3 and Pt(0.1)/Ni(12)/CeO_2(15)/MgO(2)/Al_2O_3 after reduction, reaction, and regeneration. The average particle size of Ni metal on Pt(0.1)/Ni(12)/CeO_2(15)/Al_2O_3 after the reduction was estimated to be 18.7 nm. The reaction and the regeneration increased the particle size of 25.1 nm and 30.5 nm, respectively. This behavior indicates that the Ni metal particles are aggregated gradually in each treatment step. It is characteristic that the peak assigned to Ni metal on Pt(0.1)/Ni(12)/CeO_2(15)/MgO(2)/Al_2O_3 after the reduction was much smaller than that on Pt(0.1)/Ni(12)/CeO_2(15)/Al_2O_3. This suggests that much smaller Ni metal particles are majorly present on the catalyst surface. The peak grew after the reaction, and the Ni metal particles aggregated to some extent. But the regeneration reproduced the very small, broad XRD peak, suggesting the re-dispersion of the aggregated particles.

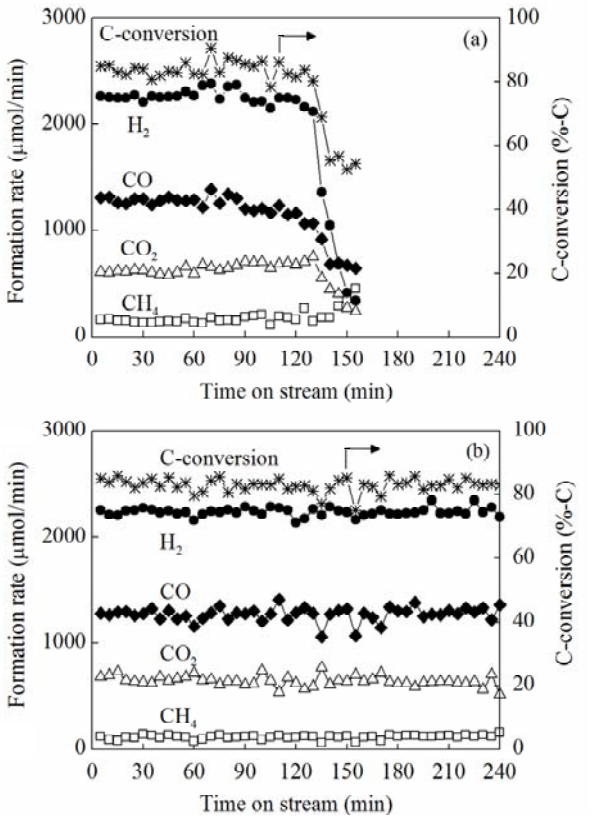

Fig. 12. Catalytic performance in steam reforming of tar with time on stream over (a) Pt(0.1)/Ni(12)/CeO_2(15)/Al_2O_3 (CI) and (b) Pt(0.1)/Ni(12)/CeO_2(15)/MgO(2)/Al_2O_3 (CI) [31]. Conditions: biomass, 60 mg/min (H_2O, 9.2%; C, 2191 μmol/min; H, 3543 μmol/min; O, 1475 μmol/min); steam, 1110 μmol/min, (added H_2O)/C = 0.5; reaction temperature, 923 K; catalyst, 1.0 g; H_2 reduction at 773 K for 30 min.

5 Steam reforming of tar over Ni/MnO/Al_2O_3 [32]

From the above results, it is concluded that the interaction of Ni and CeO_2 promoted the steam reforming of tar, especially by the activation of tar on Ni metal surface and the supply of oxygen atoms from the redox property of CeO_2. Here, we attempted the replacement of CeO_2 with other redox species such as Mn oxides. Ni/MnO_x/Al_2O_3 (CI) was

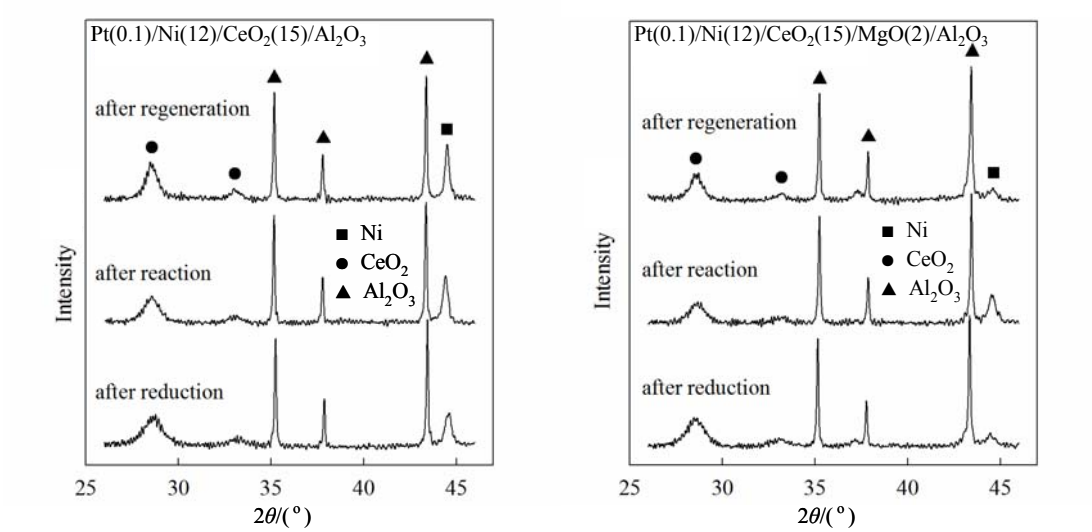

Fig. 13. XRD patterns of Pt(0.1)/Ni(12)/CeO_2(15)/Al_2O_3 and Pt(0.1)/Ni(12)/CeO_2(15) /MgO(2)/Al_2O_3 after reduction, reaction (Fig. 12), and regeneration (calcination at 873 K and reduction at 773 K) [31].

prepared by the co-impregnation method using the mixed aqueous solution of $Ni(NO_3)_2{\cdot}6H_2O$ and $Mn(NO_3)_2{\cdot}6H_2O$ in a similar way to that of Ni/CeO_2/Al_2O_3 (CI) [32]. The loading amounts of Ni and MnO are described in parentheses as mass percent on the catalyst.

Figure 14 compares the catalytic performance in steam reforming of tar over Ni(12)/MnO(20)/Al_2O_3 and Ni(12)/CeO_2(15)/Al_2O_3 catalysts. The activity of Ni(12)/MnO(20)/Al_2O_3 was so high that the tar was almost completely converted at all reaction temperatures. On the other hand, the activity of Ni(12)/CeO_2(15)/Al_2O_3 was not so high as that of Ni(12)/MnO/(20)/Al_2O_3, and the residual tar was detected at 823 K, although almost no tar was observed above 873 K. In addition, at each reaction temperature, the order of the resistance to coke formation was Ni(12)/MnO(20)/Al_2O_3 > Ni(12)/CeO_2(15)/Al_2O_3. These results indicate that the additive effect of MnO was more significant than that of CeO_2. The promoting effect of MnO_x addition can be explained in a similar way as that of CeO_2 addition, that is, the oxygen atoms derived from MnO_x species can be supplied to the Ni species to promote the reaction between carbonaceous species on Ni and oxygen species [32].

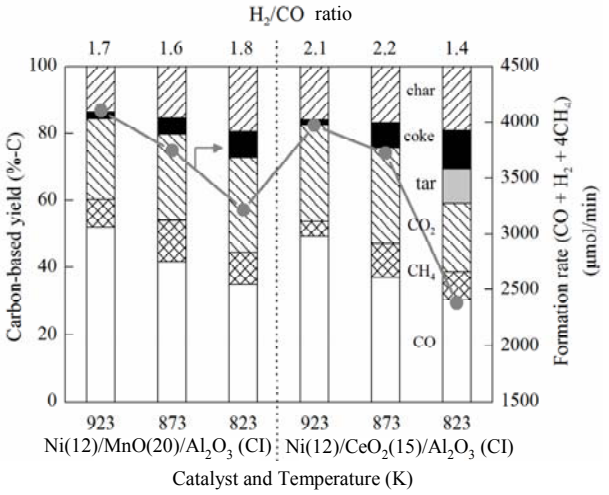

Fig. 14. Comparison of catalytic performance in steam reforming of tar over Ni(12)/MnO(20)/Al_2O_3 (CI) and Ni(12)/CeO_2(15)/Al_2O_3 (CI) [32]. Conditions: biomass, 60 mg/min (H_2O, 9.2%; C, 2191 μmol/min; H, 3543 μmol/min; O, 1475 μmol/min); steam, 1110 μmol/min, (added H_2O)/C = 0.5; catalyst, 0.5 g; H_2 reduction, 773 K, 30 min. Loading amount: Ni, 12 wt%; MnO_2, 20 wt%; CeO_2, 15 wt%.

6 Conclusions

The Ni catalyst supported on CeO_2 was effective to the suppression of coke deposition in the steam reforming of tar, and this property can be related to the Ni on CeO_2 with high reducibility. The addition of CeO_2 to Ni/Al_2O_3 by the co-impregnation method led to strong interaction between Ni metal and CeO_2 by the formation of Ni-CeO_2 nanocomposite structure. This Ni/CeO_2/Al_2O_3 catalyst showed high activity and resistance to coke deposition in the steam reforming of tar. The addition of a small amount of Pt to Ni/CeO_2/Al_2O_3 promoted the catalyst reducibility, and the catalyst was reduced with tar and steam easily. Further addition of MgO to Pt/Ni/CeO_2/Al_2O_3 enabled the re-dispersion of the aggregated Ni particles via NiO-MgO solid solution formation and its reduction. High performance of Ni-CeO_2 by the redox property of CeO_2 suggests the potential of other oxides such as manganese oxides. It is found that manganese oxides are also an effective additive on the Ni catalysts for the steam reforming of tar. In the development of the catalysts for the steam reforming of tar, the optimization of the additives and their composition is important, and

this can give various functions including high activity, stability, self-activation, and self-regeneration properties to catalysts.

References

1 Mckendry P. *Bioresour Technol*, 2002, **83**: 55
2 Huber G W, Iborra S, Corma A. *Chem Rev*, 2006, **106**: 4044
3 Wang L J, Weller C L, Jones D D, Hanna M A. *Biomass Bioenerg*, 2008, **32**: 573
4 de Lasa H, Salaices E, Mazumder J, Lucky R. *Chem Rev*, 2011, **111**: 5404
5 Baker E G, Mudge L K, Brown M D. *Ind Eng Chem Res*, 1987, **26**: 1335
6 Aznar M P, Corella J, Delgado J, Lahoz J. *Ind Eng Chem Res*, 1993, **32**: 1
7 Aznar M P, Caballero M A, Gil J, Martín J A, Corella J. *Ind Eng Chem Res*, 1998, **37**: 2668
8 Marquevich M, Czernik S, Chornet E, Montané D. *Energy Fuels*, 1999, **13**: 1160
9 Czernik S, French R, Feik C, Chornet E. *Ind Eng Chem Res*, 2002, **41**: 4209
10 Bangala D N, Abatzoglou N, Martin J P, Chornet E. *Ind Eng Chem Res*, 1997, **36**: 4184
11 Li J F, Liu J J, Liao S Y, Yan R. *Int J Hydrogen Energy*, 2010, **35**: 7399
12 Li J F, Xiao B, Yan R, Xu X R. *Bioresour Technol*, 2009, **100**: 5295
13 Wang T J, Chang J, Cui X Q, Zhang Q, Fu Y. *Fuel Process Technol*, 2006, **87**: 421
14 Le D D, Xiao X B, Morishita K, Takarada T. *J Chem Eng Jpn*, 2009, **42**: 51
15 Xiao X B, Meng X L, Le D D, Takarada T. *Bioresour Technol*, 2011, **102**: 1975
16 Wang D, Yuan W Q, Ji W. *Appl Energy*, 2011, **88**: 1656
17 Corujo A, Yermán L, Arizaga B, Brusoni M, Castiglioni J. *Biomass Bioenerg*, 2010, **34**: 1695
18 Asadullah M, Ito S-I, Kunimori K, Yamada M, Tomishige K. *J Catal*, 2002, **208**: 255
19 Asadullah M, Miyazawa T, Ito S-I, Kunimori K, Yamada M, Tomishige K. *Appl Catal A*, 2003, **255**: 169
20 Asadullah M, Miyazawa T, Ito S-I, Kunimori K, Yamada M, Tomishige K. *Appl Catal A*, 2004, **267**: 95
21 Asadullah M, Fujimoto K, Tomishige K. *Ind Eng Chem Res*, 2001, **40**: 5894
22 Asadullah M, Ito S-I, Kunimori K, Yamada M, Tomishige K. *Environ Sci Technol*, 2002, **36**: 4476
23 Asadullah M, Miyazawa T, Ito S-I, Kunimori K, Tomishige K. *Appl Catal A*, 2003, **246**: 103
24 Tomishige K, Asadullah M, Kunimori K. *Catal Today*, 2004, **89**: 389
25 Asadullah M, Miyazawa T, Ito S-I, Kunimori K, Koyama S, Tomishige K. *Biomass Bioenerg*, 2004, **26**: 269
26 Miyazawa T, Kimura T, Nishikawa J, Kado S, Kunimori K, Tomishige K. *Catal Today*, 2006, **115**: 254
27 Tomishige K, Kimura T, Nishikawa J, Miyazawa T, Kunimori K. *Catal Commun*, 2007, **8**: 1074
28 Kimura T, Miyazawa T, Nishikawa J, Kado S, Okumura K, Miyao T, Naito S, Kunimori K, Tomishige K. *Appl Catal B*, 2006, **68**: 160
29 Nishikawa J, Miyazawa T, Nakamura K, Asadullah M, Kunimori K, Tomishige K. *Catal Commun*, 2008, **9**: 195
30 Nishikawa J, Nakamura K, Asadullah M, Miyazawa T, Kunimori K, Tomishige K. *Catal Today*, 2008, **131**: 146
31 Nakamura K, Miyazawa T, Sakurai T, Miyao T, Naito S, Begum N, Kunimori K, Tomishige K. *Appl Catal B*, 2009, **86**: 36
32 Koike M, Ishikawa C, Li D L, Wang L, Nakagawa Y, Tomishige K. *Fuel*, in press, doi: 10.1016/j.fuel.2012.01.073
33 Wang L, Li D L, Koike M, Koso S, Nakagawa Y, Xu Y, Tomishige K. *Appl Catal A*, 2011, **392**: 248
34 Li D L, Wang L, Koike M, Nakagawa Y, Tomishige K. *Appl Catal B*, 2011, **102**: 528
35 Tanaka H, Kaino R, Okumura K, Kizuka T, Nakagawa Y, Tomishige K. *Appl Catal A*, 2010, **378**: 175
36 Tanaka H, Kaino R, Nakagawa Y, Tomishige K. *Appl Catal A*, 2010, **378**: 187
37 Naito S, Tanaka H, Kado S, Miyao T, Naito S, Okumura K, Kunimori K, Tomishige K. *J Catal*, 2008, **259**: 138
38 Koso S, Furikado I, Shimao A, Miyazawa T, Kunimori K, Tomishige K. *Chem Commun*, 2009: 2035
39 Koso S, Ueda N, Shinmi Y, Okumura K, Kizuka T, Tomishige K. *J Catal*, 2009, **267**: 89
40 Shinmi Y, Koso S, Kubota T, Nakagawa Y, Tomishige K. *Appl Catal B*, 2010, **94**: 318
41 Chen K Y, Koso S, Kubota T, Nakagawa Y, Tomishige K. *ChemCatChem*, 2010, **2**: 547
42 Amada Y, Koso S, Nakagawa Y, Tomishige K. *ChemSusChem*, 2010, **3**: 728
43 Ishida Y, Ebashi T, Ito S-I, Kubota T, Kunimori K, Tomishige K. *Chem Commun*, 2009: 5308
44 Ebashi T, Ishida Y, Nakagawa Y, Ito S-I, Kubota T, Tomishige K. *J Phy Chem C*, 2010, **114**: 6518
45 Bartholomew C H, Pannell R B, Butler J L. *J Catal*, 1980, **65**: 335
46 Arena F, Horrell B A, Cocke D L, Parmaliana A, Giordano N. *J Catal*, 1991, **132**: 58
47 Yamazaki O, Tomishige K, Fujimoto K. *Appl Catal A*, 1996, **136**: 49
48 Tomishige K, Chen Y G, Fujimoto K. *J Catal*, 1999, **181**: 91
49 Nurunnabi M, Mukainakano Y, Kado S, Li B T, Kunimori K, Suzuki K, Fujimoto K, Tomishige K. *Appl Catal A*, 2006, **299**: 145
50 Miyazawa T, Okumura K, Kunimori K, Tomishige K. *J Phys Chem C*, 2008, **112**: 2574
51 Chen Y G, Tomishige K, Yokoyama K, Fujimoto K. *Appl Catal A*, 1997, **165**: 335
52 Li D L, Nakagawa Y, Tomishige K. *Appl Catal A*, 2011, **408**: 1
53 Li B T, Kado S, Mukainakano Y, Miyazawa T, Miyao T, Naito S, Okumura K, Kunimori K, Tomishige K. *J Catal*, 2007, **245**:

144

54 Tomishige K, Kanazawa S, Sato M, Ikushima K, Kunimori K. *Catal Lett*, 2002, **84**: 69

55 Li B T, Kado S, Mukainakano Y, Nurunnabi M, Miyao T, Naito S, Kunimori K, Tomishige K. *Appl Catal A*, 2006, **304**: 62

56 Mukainakano Y, Li B T, Kado S, Miyazawa T, Okumura K, Miyao T, Naito S, Kunimori K, Tomishige K. *Appl Catal A*, 2007, **318**: 252

57 Miyata T, Li D L, Shiraga M, Shishido T, Oumi Y, Sano T, Takehira K. *Appl Catal A*, 2006, **310**: 97

58 Li D L, Atake I, Shishido T, Oumi Y, Sano T, Takehira K. *J Catal*, 2007, **250**: 299

59 Li D L, Shishido T, Oumi Y, Sano T, Takehira K. *Appl Catal A*, 2007, **332**: 98

60 Li D L, Nishida K, Zhan Y Y, Shishido T, Oumi Y, Sano T, Takehira K. *Appl Catal A*, 2008, **350**: 225

61 Nurunnabi M, Li B T, Kunimori K, Suzuki K, Fujimoto K-I, Tomishige K. *Catal Lett*, 2005, **103**: 277

62 Nurunnabi M, Li B T, Kunimori K, Suzuki K, Fujimoto K-I, Tomishige K. *Appl Catal A*, 2005, **292**: 272

63 Nurunnabi M, Mukainakano Y, Kado S, Miyazawa T, Okumura K, Miyao T, Naito S, Suzuki K, Fujimoto K-I, Kunimori K, Tomishige K. *Appl Catal A*, 2006, **308**: 1